賞　　状

松医会奨励賞

清水 政幸 殿

論文名

Carbon Nanotubes Induce Bone Calcification by Bidirectional Interaction with Osteoblasts

あなたは　松医会が主催する平成26年度懸賞論文において　厳正な審査の結果　頭書の成績を収めました

よって　その優れた論文を讃え　本状並びに賞金を贈り　この栄誉を賞します

平成27年5月23日

松医会

会長 勝山　努

ADVANCED MATERIALS
www.advmat.de

www.MaterialsViews.com

Carbon Nanotubes Induce Bone Calcification by Bidirectional Interaction with Osteoblasts

*Masayuki Shimizu, Yasuhiro Kobayashi, Toshihide Mizoguchi, Hiroaki Nakamura, Ichiro Kawahara, Nobuyo Narita, Yuki Usui, Kaoru Aoki, Kazuo Hara, Hisao Haniu, Nobuhide Ogihara, Norio Ishigaki, Koichi Nakamura, Hiroyuki Kato, Masatomo Kawakubo, Yoshiko Dohi, Seiichi Taruta, Yoong Ahm Kim, Morinobu Endo, Hidehiro Ozawa, Nobuyuki Udagawa, Naoyuki Takahashi, and Naoto Saito**

Carbon nanotubes (CNTs)[1,2] are a relatively new structural and conductive material that is under development in various fields.[3–6] In the field of medicine, the development and utilization of new biomaterials based on CNTs to aid treatment and diagnosis is an area of active research. Much research is now underway to use CNTs for the treatment of cancer by using them as drug delivery systems and to image cancer cells in vivo.[7–11] Researchers are also using CNTs in implanted prostheses by combining them with existing biomaterials and thereby improve their mechanical strength and endurance.[12,13] Furthermore, much attention is being focused on the use of CNTs as scaffolds for regenerative medicine, an area that has seen rapid developments in recent years.[14–18] In particular, researchers have used CNTs to facilitate bone tissue regeneration.

In 2008, we reported for the first time that bone formation was promoted by using CNT-combined scaffolds in experiments to regenerate bone tissue in vivo.[19] Since then, other research teams have shown similar results, confirming the validity of our approach. Some research teams have also shown that CNTs promote osteoblast function both in vitro and in vivo.[20–24] Based on these findings, CNTs exert their bioactivities, at least in part, via bone tissue and osteoblasts. However, the mechanisms underlying these effects of CNTs on bone tissue regeneration are unknown because, while the phenomenon has been reported, no studies have attempted to determine the mechanisms involved. Therefore, the aim of this study was to investigate the mechanisms by which CNTs promote bone formation. Here, we focused on their unique effects on calcification by osteoblasts and identified bidirectional interactions between CNTs and cells.

We first investigated the effect of CNTs on calcification of bone tissue in an experiment to test bone formation in vivo. Multi-walled (MW) CNTs with a mean diameter and length of 80 nm and 10 μm, respectively, were used in this experiment. Pellets were created by combining 2 mg of type I atelocollagen with 500 μg of MWCNTs and then mixing it with 5 μg of recombinant human bone morphogenetic protein-2 (rhBMP-2). As a control, pellets were also created by mixing MWCNT-free collagen with the same amount of rhBMP-2. To test ectopic bone formation, a pocket was made beneath the back muscle fascia of 6-week-old male ddY mice, and a MWCNT or control pellet was implanted into the pocket. The mice underwent micro-computed tomography (μ-CT) on Day 10 after implantation, at which time calcification has started to occur in the first stage of ectopic bone formation, and on Day 21, at which time calcification is near complete.[25] On Day 10, slight bone formation was

Prof. N. Saito
Department of Applied Physical Therapy
Shinshu University School of Health Sciences
Asahi 3-1-1, Matsumoto
Nagano 3908621, Japan
E-mail: saitoko@shinshu-u.ac.jp
Dr. M. Shimizu, Dr. N. Narita, Dr. K. Aoki, Dr. K. Hara, Dr. N. Ogihara, Dr. N. Ishigaki, Dr. K. Nakamura, Prof. H. Kato
Department of Orthopaedic Surgery
Shinshu University School of Medicine
Asahi 3-1-1, Matsumoto 3908621, Japan
Dr. Y. Kobayashi, Dr. T. Mizoguchi, Prof. H. Nakamura, Dr. I. Kawahara, Prof. H. Ozawa, Prof. N. Takahashi
Institute for Oral Science
Matsumoto Dental University
Hirooka Gobara 1780, Shiojiri 3900781, Japan
Dr. Y. Usui
Research Center for Exotic Nanocarbons
Shinshu University
Wakasato 4-17-1, Nagano 3808553, Japan
Dr. H. Haniu
Institute of Carbon Science and Technology
Shinshu University
Wakasato 4-17-1, Nagano 3808553, Japan
Dr. M. Kawakubo
Department of Laboratory Medicine
Shinshu University Hospital
Asahi 3-1-1, Matsumoto 3908621, Japan
Dr. Y. Dohi
Department of Public Health
Health Management and Policy
Nara Medical University School of Medicine
Shijo-cho Kashihara 840, Nara 6348521, Japan
Prof. S. Taruta, Dr. Y. A. Kim, Prof. M. Endo
Faculty of Engineering
Shinshu University
Wakasato 4-17-1, Nagano 3808553, Japan
Prof. N. Udagawa
Department of Biochemistry
Matsumoto Dental University
Hirooka Gobara 1780, Shiojiri 3900781, Japan

DOI: 10.1002/adma.201103832

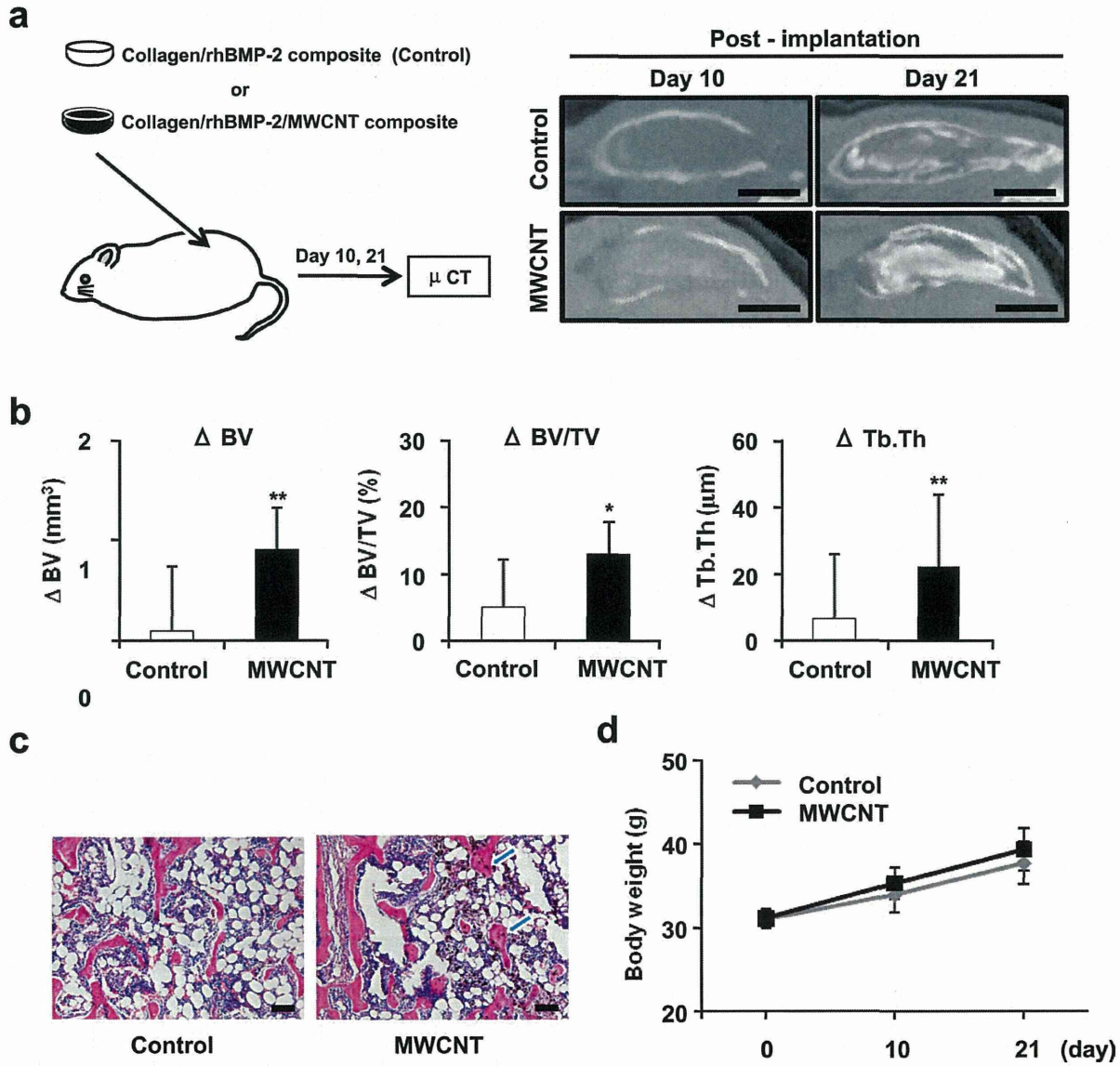

Figure 1. MWCNTs promote calcification during rhBMP-2-induced ectopic bone formation in mice. a) Pellets were created by combining 2 mg of type I atelocollagen with 500 μg of MWCNTs or MWCNT-free collagen, followed by mixing with 5 μg of rhBMP-2. The pellets were then implanted in a back muscle pocket in ddY mice. The mice underwent μ-CT on Days 10 and 21 after implantation. On Day 10, some bone had formed in both groups of mice, but there was no difference in the extent of calcification between the two groups. By contrast, on Day 21, greater bone formation was detected in the MWCNT group than in the control group. Scale bars, 2 mm. b) 3D morphometric analysis of μ-CT images was performed to determine the bone volume (BV, mm^3), tissue volume (TV, mm^3), and trabecular thickness (Tb.Th, μm) on Days 10 and 21. The increments in three parameters (BV, BV/TV and Tb.Th) were significantly greater in the MWCNT group than in the control group. $*P < 0.05$, $**P < 0.01$ compared with control. Error bars are standard deviation (s.d.) In the histological images acquired on Day 21, better new bone formation was observed in the MWCNT group than in the control group. In the MWCNT group, MWCNT particles (blue arrows) were incorporated into new bone trabeculae. Haematoxylin and eosin staining. Scale bars: 50 μm. d) The body weight of mice was measured at implantation, and at Days 10 and 21. There was no difference between the MWCNT and control groups in terms of changes in body weight at either Day 10 or 21 relative to that at implantation. Error bars are s.d.

observed in both groups of mice and there was no difference between the groups. On Day 21, μ-CT showed that bone formation was significantly greater in the MWCNT group than in the control group (**Figure 1**a).

Three-dimensional morphometric analysis of the μ-CT images was performed to determine bone volume (BV), tissue volume (TV) and trabecular thickness (Tb.Th) on Days 10 and 21. The increments in three parameters (BV, BV/TV and Tb.Th) were significantly greater in the MWCNT group than in the control group (Figure 1b). In the histological images acquired on Day 21, new bone tissues consisted of normal-appearing trabeculae and haematopoietic marrow in both groups, but

better bone formation was observed in the MWCNT group than in the control group. In addition, the MWCNT particles were incorporated entirely into new bones, directly contacting the bone matrix in trabeculae (Figure 1c). There was no difference between the two groups of mice with respect to changes in body weight during the experimental period (Figure 1d). These results suggest that MWCNTs promote calcification during ectopic bone formation induced by rhBMP-2.

To elucidate the mechanism by which MWCNTs promote calcification in vivo, we examined the effects of MWCNTs on calcification by osteoblasts in vitro. Osteoblast-like stromal cells were collected from the calvaria of 1-day-old mice and cultured. After 2 days of culture, MWCNTs were added at concentrations of 0.5, 5 or 50 μg mL^{-1}. The cells were cultured for 3 weeks and then stained with alizarin red S (alizarin). As a comparator, cells were treated with 0.5, 5 or 50 μg mL^{-1} of conventional carbon black (CB), carbon nanoparticles with a mean diameter of 80 nm. To disperse the MWCNT or CB particles, carboxymethylcellulose (CMC) was added at a concentration (2 μg mL^{-1}), which did not affect cell viability (data not shown). A culture medium without carbon particles but containing CMC was used as a control. After cell culture for 3 weeks, the degree of calcification was negligible in both the control and CB-treated groups, but was much higher in the 50 μg mL^{-1} MWCNT group. When cells were cultured for 6 weeks and stained with alizarin, calcification was observed in the control and CB groups, but the degree of calcification was higher in the MWCNT groups (**Figure 2**a).

When alizarin staining was quantified using imaging software, the area of calcification was significantly greater in the 50 μg mL^{-1} MWCNT group than in the CB groups at Week 3. In addition, the area of calcification increased in a concentration-dependent manner in both the MWCNT and CB groups at Week 6. At this point, the area of calcification was significantly greater in the 50 μg mL^{-1} MWCNT group than in the CB groups (Figure 2b).

In the MWCNT-treated groups, scanning electron microscopy (SEM) showed the presence of small nodules and spherical crystals around the MWCNTs that were located near osteoblasts (Figure 2c). Transmission electron microscopy (TEM) showed that needle-like crystals had precipitated around the MWCNTs. Electron energy loss spectroscopy (EELS) showed the needle-like crystals contained abundant calcium. The diffraction pattern and its intensity profile in the area containing only needle-like crystals without the MWCNTs were almost consistent with the known peak of hydroxyapatite (HA), showing that the calcified substance stained with alizarin was almost identical to HA crystals (Figure 2d). Thus, MWCNTs promoted calcification caused by HA formation in the presence of osteoblasts.

To test whether the calcification associated with MWCNTs was dependent on osteoblasts, culture media containing MWCNTs and CB but not osteoblasts were stained with alizarin after incubation for 3 and 6 weeks, as described above. In this experiment, no calcification was observed in any of the groups (Figure 2e), indicating that the calcification-promoting effects of MWCNTs required osteoblasts and that HA was not crystallized by MWCNTs in the absence of osteoblasts.

Next, we investigated the effects of MWCNTs on osteoblast proliferation and differentiation. Osteoblasts were incubated with 50 μg mL^{-1} MWCNTs or CB for up to 8 days and proliferative activity was determined at 1, 3, 5, and 8 days by the Alamar Blue assay. There were no differences between the MWCNT or CB group and the control group, confirming that MWCNTs did not influence the proliferation of osteoblasts (**Figure 3**a).

The effects of MWCNTs on the differentiation of osteoblast-like stromal cells to mature osteoblasts were also investigated. Primary cultured osteoblast-like stromal cells were incubated with 50 μg mL^{-1} of MWCNTs or CB. After 1 and 5 days, total RNA was extracted and the mRNA expression of two phenotypic osteoblast markers, *osteocalcin* (a bone matrix protein) and *Runx 2* (an essential transcription factor for osteoblast differentiation),[26–28] was quantified by real-time RT-PCR. The expression of *Runx 2*, an early marker of differentiation, was measured on Day 1, and that of *osteocalcin*, a late marker of differentiation, was measured on Day 5. The expression of *Runx 2* tended to be higher in the MWCNT group than in the control and CB groups, although these differences were not statistically significant. The expression of *osteocalcin* was significantly higher in the MWCNT group than in the control and CB groups (Figure 3b). Based on these findings, MWCNTs affected osteoblasts by promoting the differentiation of undifferentiated osteoblasts to mature osteoblasts.

To elucidate the mechanism by which the MWCNTs promoted osteoblast differentiation, we investigated the effects of MWCNTs on Ca accumulation around the osteoblasts. First, 0.5, 5, or 50 μg mL^{-1} of MWCNTs or 50 μg mL^{-1} of CB was added to a culture medium without osteoblasts. After 1 week, the culture medium was removed and the bottom surface of each plate was scraped. Ca that accumulated on the bottom of the plate was extracted using formic acid and quantified. The Ca content on the bottom of the plate increased in a concentration-dependent manner in the MWCNT groups. Furthermore, the Ca content was significantly greater in the 50 μg mL^{-1} MWCNT group than in the 50 μg mL^{-1} CB and control groups (CMC alone) (**Figure 4**a). This suggests that MWCNTs attracted Ca in the culture media and increased the Ca content on the bottom of the plate.

Next, we determined whether osteoblast differentiation was influenced by the accumulation of Ca. Osteoblasts were cultured for 5 days in culture media containing 100 mg L^{-1}, 200 mg L^{-1} or 400 mg L^{-1} Ca, and were stained for alkaline phosphatase (ALP). ALP staining intensity increased in a Ca concentration-dependent manner (Figure 4b).

Next, osteoblasts were cultured in culture media containing different Ca concentrations, and total RNA was extracted on Days 1 and 5 to determine the expression of *Runx 2* (Day 1) and *osteocalcin* (Day 5) by real-time RT-PCR. The expression of *Runx 2* and *osteocalcin* increased in a Ca concentration-dependent manner and was significantly greater in cells exposed to 200 mg L^{-1} Ca and 400 mg L^{-1} Ca than in cells exposed to 100 mg L^{-1} Ca (Figure 4c), indicating that osteoblast differentiation was promoted by increasing Ca concentration. Taken together, these results suggest that MWCNTs enhance Ca accumulation around osteoblasts and induce their differentiation.

Of the many enzymes produced by osteoblasts, ALP is the most widely used marker for osteoblast activation. ALP plays an important role in calcification during bone formation and our findings indicate that osteoblasts are responsible for calcification

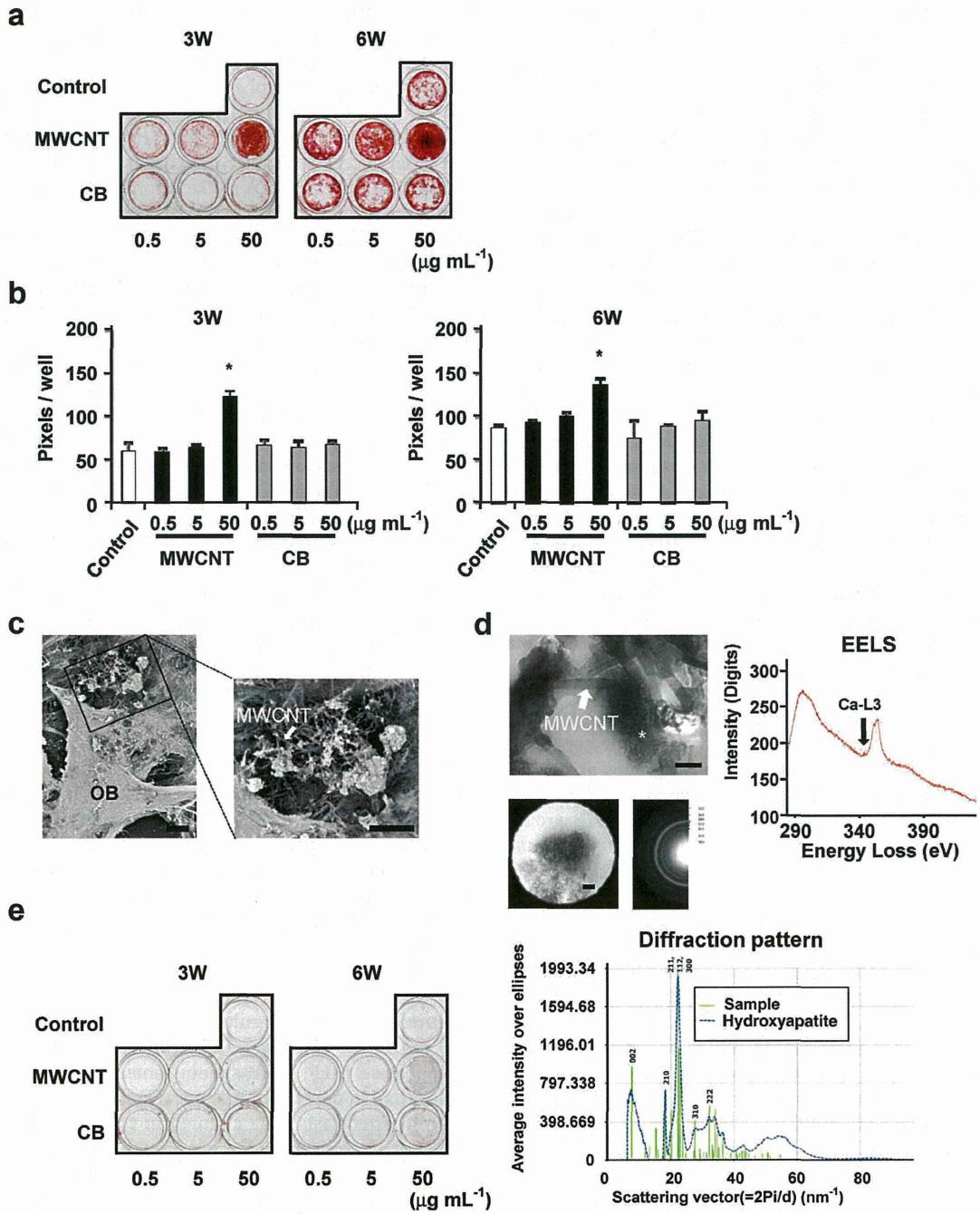

Figure 2. MWCNTs promote calcification during HA formation by osteoblasts. a) Primary cultured osteoblasts were incubated with 0.5, 5, or 50 μg mL^{-1} MWCNTs or CB. After culture for 3 weeks, the degree of calcification was very low in the control (no carbon particles) and CB groups, and high in the 50 μg mL^{-1} MWCNT group. By Week 6, calcification was observed in the control and CB groups, but the degree of calcification was higher in the MWCNT groups (alizarin staining). b) The area of calcification determined by image analysis was significantly greater in the 50 μg mL^{-1} MWCNT group than in the CB groups at Week 3. Although the area of calcification increased in a concentration-dependent manner in both the MWCNT and CB groups at Week 6, the area of calcification was significantly greater in the 50 μg mL^{-1} MWCNT-treated group than in the CB-treated groups. $*P < 0.01$ compared with CB at the same concentration. Error bars are s.d. c) SEM showed small nodules and spherical crystals around the MWCNTs located near osteoblasts (OB). Scale bars, 5 μm. d) TEM showed needle-like crystals (*) around the MWCNTs. The localization of Ca was determined by energy filtering TEM. EELS enabled obtainment of high-resolution Ca-sensitive images using ionization edge loss electrons. The edge of electron energy loss spectra indicated Ca-L3 localization. We then investigated the diffraction patterns of samples (samples from the area containing only crystals without the MWCNTs). A selected area diffraction pattern and its intensity profile revealed that the peak of the crystals almost coincided with the known peak of HA. Scale bars, 100 nm. e) No calcification occurred when MWCNTs or CB were added to culture media lacking osteoblasts (alizarin staining).

ADVANCED MATERIALS
www.advmat.de

www.MaterialsViews.com

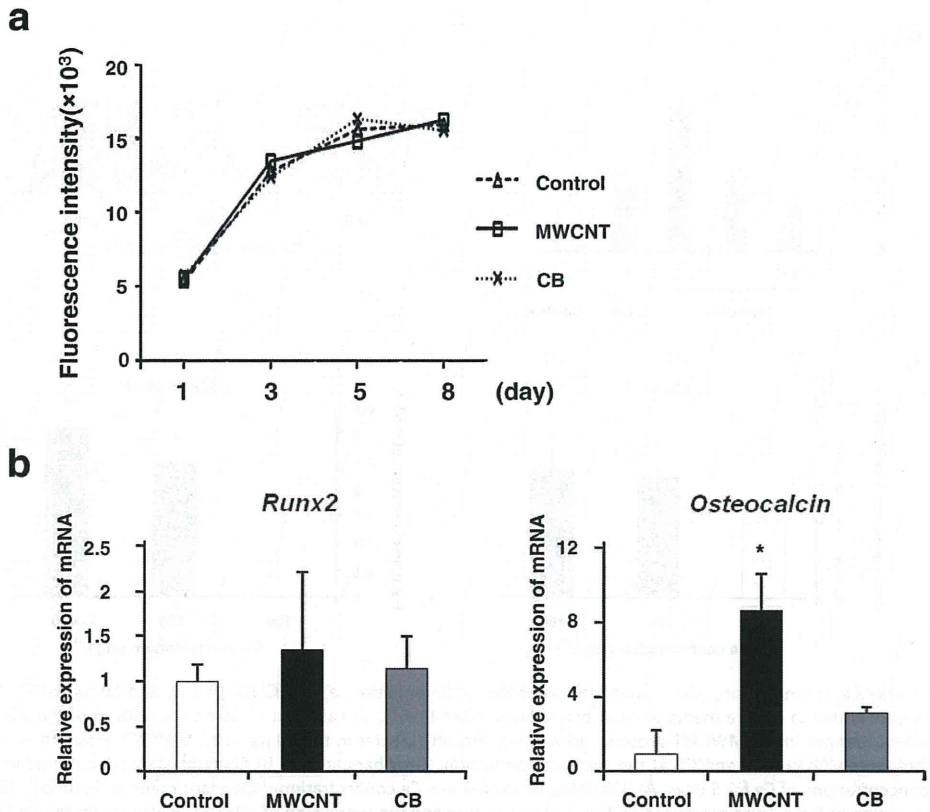

Figure 3. Effects of MWCNTs on osteoblast proliferation and differentiation. a) 50 μg mL^{-1} MWCNTs or CB were added to the osteoblast culture media and the cells were cultured for up to 8 days. There was no difference in proliferative capacity between the two groups and the control group on Days 1, 3, 5, or 8 (Alamar blue assay). b) Primary cultured osteoblast-like stromal cells were incubated with 50 μg mL^{-1} MWCNTs for up to 5 days. Real-time RT-PCR was used to detect the expression of *Runx 2*, an early marker of differentiation, on Day 1, and the expression of *osteocalcin*, a late marker of differentiation, on Day 5. The expression of *Runx 2* tended to be higher in the MWCNT group than in the control and CB groups, while that of *osteocalcin* was significantly higher in the MWCNT group than in the control and CB groups. $*P < 0.01$ compared with control and CB. $*P < 0.01$. Error bars are s.d.

around MWCNTs. Therefore, we investigated whether it was possible to induce calcification around MWCNTs using ALP produced by other cells. NIH 3T3 and ST2 cell lines are fibroblast-like cells, but only ST2 cells are able to induce calcification when stimulated with rhBMP-2.[29] Therefore, NIH3T3 and ST2 cells were incubated with 50 μg mL^{-1} of MWCNTs or CB. We also treated MC3T3-E1 cells, an osteoblast-like cell line, in a similar manner. After 5 weeks, alizarin staining showed calcification of MC3T3-E1 cells treated with MWCNTs, whereas NIH3T3 and ST2 treated with MWCNTs or CB did not show calcification (**Figure 5**a). Meanwhile, ST2 cells treated with 100 ng mL^{-1} of rhBMP-2 plus MWCNTs for 3 weeks exhibited calcification, whereas those treated with rhBMP-2 plus CB did not. In contrast, calcification was not observed in NIH3T3 cells treated with 100 ng mL^{-1} of rhBMP-2, irrespective of the carbon treatment (Figure 5b).

Based on these findings, we investigated whether calcification induced by rhBMP-2 plus MWCNTs was due to the expression of ALP by ST2 cells.[30] To test this possibility, ST2 cells were cultured for 1 week with rhBMP-2 plus 0, 0.5, or 1.0 mM 3,4-dehydro-L-proline (DHP), an ALP inhibitor, in the absence of MWCNTs. ALP staining at 1 week showed a decrease in staining that was dependent on the DHP concentration (Figure 5c). Next, ST2 cells were incubated with 50 μg mL^{-1} MWCNTs, rhBMP-2 and 0, 0.5, and 1.0 mM DHP. After culture for 3 weeks, ALP activity and alizarin staining decreased in a DHP concentration-dependent manner, indicating that calcification of ST2 cells in the presence of MWCNTs and rhBMP-2 is due to the production of ALP by ST2 cells (Figure 5d). Overall, the results of this series of studies indicate that ALP-producing cells, not just osteoblasts, can induce calcification around MWCNTs, suggesting that ALP is an important factor that induces calcification around MWCNTs.

In this study, we showed that chemically unmodified MWCNTs promote bone formation by interacting with osteoblasts. We found that MWCNTs increase the concentration of Ca around osteoblasts by accumulating Ca and, when the undifferentiated osteoblasts detect the increase in Ca, they differentiate to mature osteoblasts and promote calcification. Ca adsorption on MWCNTs is thought to be due to their negative zeta potential[31,32] which attracts Ca ions. Recently, it has become evident that osteoblasts express a calcium-sensing

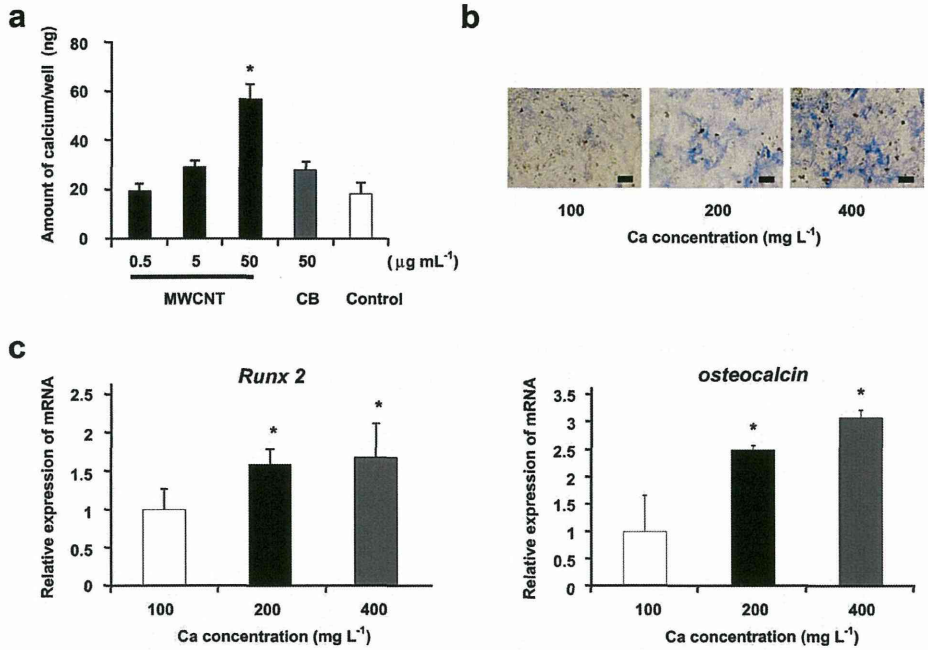

Figure 4. MWCNTs cause Ca accumulation, which promotes osteoblast differentiation. a) MWCNTs (0.5, 5, and 50 μg mL^{-1}), CB (50 μg mL^{-1}), or CMC alone (control) were added to culture media without osteoblasts. After 1 week, the amount of Ca on the bottom of the plate had increased in a concentration-dependent manner in the MWCNT groups and was significantly greater in the 50 μg mL^{-1} MWCNT group than in the CB and control groups. $*P < 0.01$ compared with control and CB at the same concentration. Error bars are s.d. b) Osteoblasts were cultured in osteogenic medium containing various concentrations of Ca for 5 days. ALP staining increased in a Ca concentration-dependent manner. Scale bar, 100 μm. c) Using real-time RT-PCR, the expression of *Runx 2* was measured on Day 1 of cell culture and the expression of *osteocalcin* was measured on Day 5. The expression of both *Runx 2* and *osteocalcin* increased in a Ca concentration-dependent manner and was significantly higher in cells cultured with 200 mg L^{-1} Ca and 400 mg L^{-1} Ca than in cells cultured with 100 mg L^{-1} Ca. $*P < 0.05$ compared with 100 mg L^{-1} Ca. Error bars are s.d.

receptor (CaSR) and that osteoblast differentiation is stimulated by high extracellular Ca concentrations.[33–35] Unfortunately, many of the functions of the CaSR in osteoblasts remain unknown and further studies are needed. Meanwhile, it is known that, during bone formation, a large amount of ALP is released from osteoblasts. We also found that high ALP concentrations induce calcification around MWCNTs. It has been suggested that, when MWCNTs interact with osteoblasts, calcification rapidly progresses and hence so does bone formation.

In summary, MWCNTs and osteoblasts interact bidirectionally as follows: MWCNTs promote osteoblast differentiation by attracting Ca, and differentiated osteoblasts promote calcification around MWCNTs by releasing ALP. This is the first to report bidirectional interactions between MWCNTs and cells and the advantages of these interactions conferred to living tissue. However, it must be considered that other factors may also contribute to the bone-promoting effects of MWCNTs. For example, the adhesion of cells to MWCNTs,[36] invasion of blood vessels around MWCNTs,[37] and the relationship between MWCNT molecules and collagen molecules[38] need to be studied. Nevertheless, the effects of MWCNTs on osteoblasts and the reciprocal effects of osteoblasts on MWCNTs observed in the present study are likely to contribute to bone formation by promoting calcification, an essential stage of de novo bone formation.

One of the stages of bone formation, calcification, is a key target for bone regenerative medicine and there is a need to speed up bone formation by increasing the rate of early calcification. However, there is still uncertainty about the mechanisms involved in initial calcification in bone formation, even though this has been a focus of many studies conducted over the years. Historically, the following three theories have been proposed: the booster mechanism theory,[39] the epitaxy theory,[40] and the matrix vesicle theory.[41,42] The present study revealed that elevated ALP induces calcification around MWCNTs, supporting the booster mechanism theory, which advocates the important role of ALP elevation. Our study also revealed that calcification occurs in the presence of MWCNTs, supporting the epitaxy theory, which advocates that calcification requires a substance that serves as a core. The matrix vesicle theory is a combination of these two theories, advocating that the matrix vesicles themselves serve as cores for calcification (epitaxy) when the Ca concentration in the matrix vesicles produced by osteoblasts is increased and the phosphate concentration is increased by the metabolism of pyrophosphate by ALP. MWCNTs may play a role similar to that of matrix vesicles. That is, HA crystals are formed more easily when MWCNTs cause Ca accumulation while the phosphate concentration is increased by an increase in ALP activity and the resultant degradation of β-glycerophosphate in culture media. Calcification may then occur when MWCNTs as small

ADVANCED MATERIALS
www.advmat.de

www.MaterialsViews.com

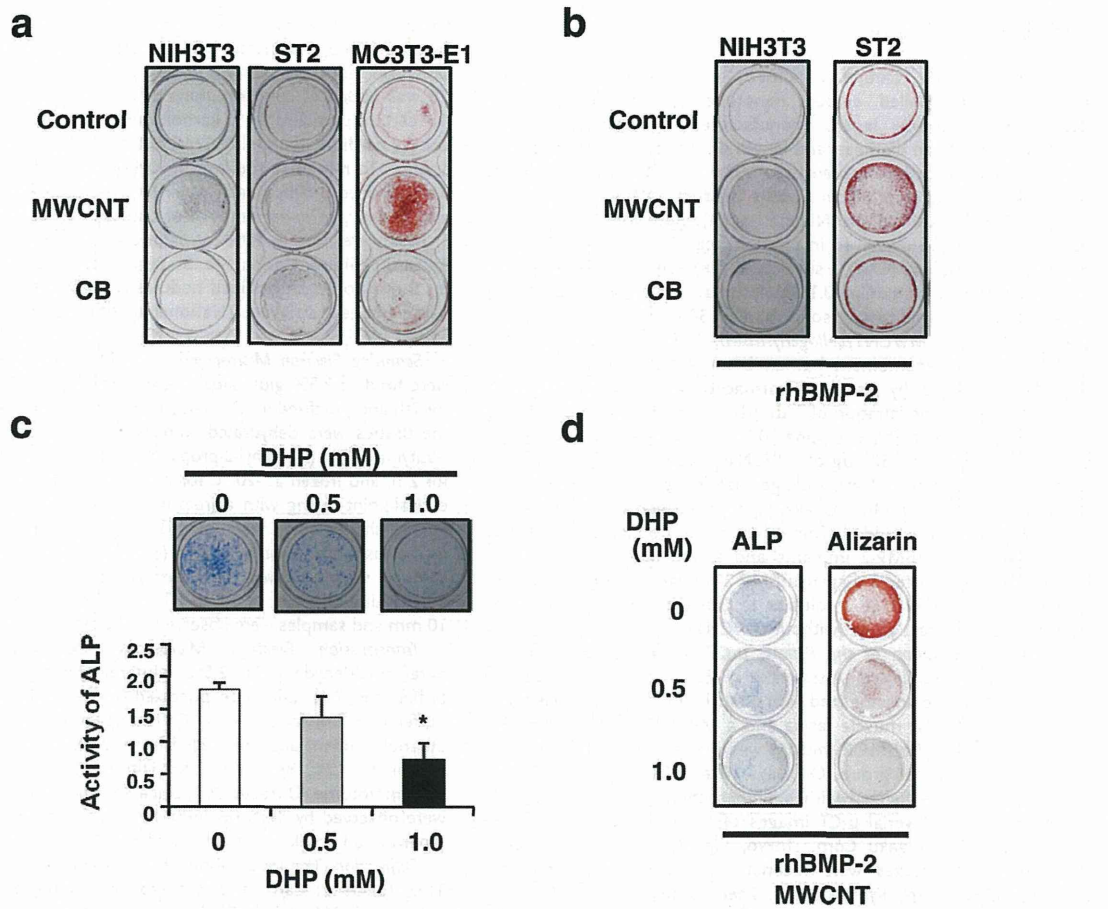

Figure 5. Role of ALP expressed in non-osteoblast cells on calcification around MWCNTs. a) Fibroblast-like cell lines (NIH3T3 and ST2) and an osteoblast-like cell line (MC3T3-E1) were cultured with 50 μg mL^{-1} MWCNTs or CB. After 5 weeks, MC3T3-E1 cells treated with MWCNT, but not those treated with CB, exhibited calcification. By contrast, calcification was not observed in the NIH3T3 or ST2 cell lines, irrespective of the culture conditions (alizarin staining). b) NIH3T3 and ST2 cells were treated with 100 ng mL^{-1} rhBMP-2 as well as MWCNTs or CB. After 3 weeks, ST2 cells treated with rhBMP-2 plus MWCNTs exhibited calcification, whereas those treated with rhBMP-2 plus CB did not. None of the groups of NIH3T3 cells exhibited calcification. c) ST2 cells were treated with rhBMP-2 plus 0, 0.5 or 1.0 mM DHP, an ALP inhibitor. After 1 week, DHP decreased ALP staining and activity in a concentration-dependent manner. $*P < 0.05$ compared with 0 mM DHP. Error bars are s.d. d) ST2 cells were treated with 50 μg mL^{-1} MWCNT, rhBMP-2 and 0, 0.5, or 1.0 mM DHP. After 3 weeks, DHP decreased ALP staining and calcification (alizarin staining) in a concentration-dependent manner.

as matrix vesicles (diameter: 40–200 nm) serve as an epitaxy. We believe that further research into the interactions between MWCNTs and osteoblasts will lead to the identification of the, still unknown, mechanisms underscoring bone calcification, the discovery of methods to enhance bone formation and, ultimately, significant breakthroughs in bone regenerative medicine.

So far, some biomaterials have been shown to interact with and activate living tissues, and induce reactions that are advantageous to living organisms. These biomaterials have unidirectional activity and most of them are used because of their biodegradable nature.[43] Of interest, the interactions between MWCNTs and cells shown in the present study were not due to their biodegradability. The main limitation of conventional bioactive materials is that their characteristics change over time because of their biodegradability, leading to the loss of mechanical strength, for example. MWCNTs have the potential to offer a completely new biomaterial that shows prolonged bioactivity coupled with their original characteristics. A major reason for the bidirectional activity of MWCNTs is that they are nanosized structures with a similar size to intracellular organelles. In terms of bone formation, MWCNTs have a similar size to the matrix vesicles released from osteoblasts. The reaction between nanosized materials and living organisms at the cellular and molecular levels is a rapidly evolving area of research.[44–46] Many previously unknown phenomena have been reported and more are expected to be discovered.[47,48] A search for reactions that are advantageous to living organisms, such as the bidirectional interactions between nanomaterials and cells shown in the present study, will allow us to develop innovative biomaterials that will have a major impact on future medicine.

Experimental Section

Carbon Materials: Carbon nanotubes used in the study were commercial multi-walled carbon nanotubes (MWCNTs) (VGCF-S; Showa Denko, Tokyo, Japan) manufactured by chemical vapour deposition. The mean diameter and length of the MWCNTs were 80 nm and 10 μm, while carbon content was ≥99.9 wt%. Carbon black (CB), with a mean diameter of 80 nm, was a product for general industrial use (Asahi#50; Asahi Carbon, Niigata, Japan). Both MWCNTs and CB were autoclaved and dissolved in physiological saline containing 0.1% carboxymethylcellulose (CMC, a surfactant) for in vitro experiments or in physiological saline containing 0.1% polysorbate for in vivo experiments, and were homogenized by ultrasonication for 30 min.

Preparation of MWCNT/collagen/rhBMP-2 Pellets and Collagen/rhBMP-2 Pellets: Recombinant human bone morphogenetic protein-2 (rhBMP-2) provided by Astellas Pharmaceutical (Tokyo, Japan) was mixed, to a final concentration of 1 μg μL^{-1}, with a solution containing 5 mM glutamic acid, 2.5% glycine, 0.5% sucrose, 5 mM NaCl and 0.01% Tween 80. Next, 500 μg of MWCNTs was mixed with a solution containing 2 mg of type-I atelocollagen (atelopeptide type I collagen) (Cellmatrix; Nitta Gelatin Inc., Osaka, Japan), to which 5 μL of the above rhBMP-2 solution was added. This mixture was lyophilized to prepare MWCNT/collagen/rhBMP-2 implants and stored at -20°C until used. As a control, lyophilized collagen/rhBMP-2 implants were prepared by adding 5 μL of the rhBMP-2 solution to 2 mg of type-I atelocollagen containing polysorbate alone (without MWCNTs).

In vivo Implantation of the Pellets, μ-CT Analysis of Ectopic Bone Formation, and Histological Assessment of Ectopic Bone: Six-week-old male ddY mice were anesthetized with diethyl ether. A pocket was made beneath the left back muscle fascia and a MWCNT/collagen/rhBMP-2 implant or collagen/rhBMP-2 implant was inserted aseptically into the pocket in 17 mice per group. On Days 10 and 21 after implantation, the mice were anesthetized with sodium pentobarbital (25 mg kg^{-1}, intramuscular), and serial μ-CT images of the implantation site were acquired (R_mCT; Rigaku Corp., Tokyo, Japan) to assess new bone formation. μ-CT images were reconstructed using i-View software (J. Morita MFG. Corp., Kyoto, Japan). Then, bone volume (BV), tissue volume (TV) and trabecular thickness (Tb.Th) were determined by 3D bone morphometric analysis using TRI/3D-BON software (Ratoc System Engineering, Tokyo, Japan). New bone formation was assessed, as was calcification, by determining the increments in these parameters from Day 10 to Day 21. Mice were allowed to recover after each scan. On Day 21, the ectopic bone was removed, fixed, defatted, embedded, cut, stained with haematoxylin and eosin, and examined under a light microscope. All mice were weighed on Days 0, 10, and 21. None of the mice died during this period. Since all mice were from the same litter with identical genetic background, and were used in the experiments around the same time, the individual variation among the animals was ignorable. All procedures for animal experiments were carried out in compliance with the guidelines of the Institutional Animal Care Committee of Shinshu University.

Collagen Coating: A 48-well plate was coated with collagen to prevent the cells from shearing off from the bottom of the well during staining, as follows. First, 100 μL of acetic acid solution was added to 40 mL of Milli-Q water and sterile-filtered, followed by the addition of 4 mL of type I atelocollagen (atelopeptide type I collagen solution) (Cellmatrix; Nitta Gelatin Inc.). Next, 250 μL of this solution was added to each well of the culture plate and incubated for 5 min, and was then aspirated. The following experiments were performed using collagen-coated culture plates.

Osteoblast Culture and Detection of Calcification: Osteoblast-like stromal cells were collected from the calvaria of 1-day-old mice. All procedures for animal experiments were carried out in compliance with the guidelines of the Animal Management Committee of Matsumoto Dental University. Osteoblast-like stromal cells were cultured for 2 days in α-modified Eagle's minimum essential medium (α-MEM) (Sigma-Aldrich, Inc., St. Louis, MO, USA) containing 10% fetal bovine serum (FBS; JRH Biosciences, Lenexa, KS, USA). On Day 2, the medium was changed to α-MEM containing 100 μg mL^{-1} ascorbic acid (Nacalai Tesque, Kyoto, Japan) and 5 mM β-glycerol phosphate (Wako Pure Chemical Industries, Osaka, Japan) (osteogenic medium). MWCNTs or CB was added at concentrations of 0.5, 5, or 50 μg mL^{-1}. To disperse the carbon particles, 0.1% carboxymethylcellulose (CMC) was added. A culture medium containing CMC but no carbon materials was used as a control. To minimize the loss of carbon materials, the culture medium was replaced 3 times each week by aspirating half of the supernatant and adding the same amount of osteogenic medium. At Weeks 3 and 6, cells were fixed in 10% formalin and stained with 1% alizarin red S (alizarin) (Sigma-Aldrich, Inc. St. Louis, MO, USA) at room temperature for 5 min to detect calcified nodules. Calcified sections were quantified using Image J software (National Institute of Health, Bethesda, MD, USA).

Scanning Electron Microscopy: For SEM observation, the cultured cells were fixed in 2.5% glutaraldehyde in phosphate buffer (pH 7.4), at 4 °C for 2 h and postfixed in 2% OsO_4 in the same buffer at 4 °C for 1 h. Then, the tissues were dehydrated with an ethanol gradient, substituted with t-butyl alcohol (2-methyl-2-propanol) (Nacalai Tesque), cooled at 4 °C for 2 h, and frozen at -20 °C for 2 h. The samples were then prepared by critical-point drying with a freezing drier (JFD-310; JEOL, Tokyo, Japan). Finally, the samples were coated with OsO_4 to a thickness of 5 nm by an osmium plasma coater (OPC-40; Fligen, Nagoya, Japan). The samples were observed by field-emission SEM (JSM-7001F; JEOL) with accelerating voltages of 10 and 15 kV. The working distance (WD) was 10 mm and samples were observed in the secondary electrons (SE) mode.

Transmission Electron Microscopy: Cells were fixed in 2% paraformaldehyde and 2.5% glutaraldehyde in 0.1 M cacodylate buffer (pH 7.4), and then postfixed in 1% OsO_4 in 0.1 M cacodylate buffer (pH 7.4) for 2 h at 4 °C. The specimens were dehydrated in an ethanol gradient and embedded in resin (Epon 812; TAAB Laboratories Equipment Ltd., Berkshire, UK). Ultrathin sections were cut using an ultramicrotome (Ultracut UCT; Leica Microsystems, Vienna, Austria) and were observed by TEM (H-7600; Hitachi High-Technologies Co., Tokyo, Japan) at an accelerating voltage of 80 kV.

Diffraction: The localization of Ca was determined by energy filtering TEM (LEO912; Carl Zeiss, Oberkochen, Germany) at an accelerating voltage of 120 kV.[49] EELS enabled obtainment of high-resolution Ca-sensitive images using ionization edge loss electrons.[50] We then investigated the diffraction patterns of samples (samples from the area containing only crystals without the carbon nanotubes) and evaluated whether the Ca in samples constituted HA. Diffraction data were analysed using Process Diffraction software (Research Institute for Technical Physics and Materials Science, Head of Thin Film Physics Laboratory, Budapest, Hungary). The diffraction patterns of the samples were compared with the known pattern of HA.

Cell Proliferation Assay: Cell proliferation was assessed using an Alamar Blue assay kit (Invitrogen Corp., Carlsbad, CA, USA). Osteoblast-like stromal cells were cultured for 2 days in α-MEM containing 10% FBS. On Day 2, the culture medium was changed to osteogenic medium containing 50 μg mL^{-1} MWCNTs or CB, or with CMC alone (without carbon materials) as a control. Alamar Blue assays were performed on Days 1, 3, 5, and 8. Resazurin dye was added to a volume of 1/10 of the culture medium 4 h before measuring fluorescence intensity. To remove carbon materials, the culture media were centrifuged at 14 000 rpm for 10 min at 4 °C. The fluorescence intensity (excitation/emission, 560/590 nm) of the supernatant was measured using a spectrophotometer (SpectraMax Gemini XS; Molecular Devices, Inc., Sunnyvale, CA, USA).

Preparation of RNA and Real-Time RT-PCR: As described above, osteoblast-like stromal cells were cultured, and treated with carbon materials for 1 or 5 days. Total cellular RNA was extracted from osteoblasts using the method of Yamamoto et al.[51] cDNA was synthesized from total RNA using a reverse transcription kit (ReverTraAce, Toyobo Co., Ltd., Osaka, Japan), and two-step PCR was performed using a real-time PCR detection system (DNA Engine Opticon system; MJ Japan, Tokyo, Japan) with specific primers for *Runx 2*, *osteocalcin*, or glyceraldehyde-3-phosphate dehydrogenase (*GAPDH*, Takara Bio Inc.,

ADVANCED MATERIALS
www.advmat.de

www.MaterialsViews.com

Shiga, Japan). The fold-change ratios between test and control samples were calculated.

Determination of Ca Concentrations on the Bottom of Plates: A 48-well plate was coated with collagen as described above, and each well was filled with 250 μL of α-MEM with 10% FBS. After 2 days, the medium was changed to osteogenic medium containing MWCNTs or CB, or CMC alone. Five days later, the culture medium was carefully aspirated, and 250 mM sucrose in 10 mM Tris-HCl (pH 7.0) was added. The bottom of the plate was scraped to completely recover the precipitate, including the carbon material. The precipitate was centrifuged twice at 14 000 rpm for 10 min at 4 °C and the supernatant was discarded after both centrifugations. Ca was extracted from the precipitate using 20% formic acid by the method of Nakamura et al.[52] Calcium E test reagent (Wako Pure Chemical Industries) was added to the extract and Ca content was measured using a spectrophotometer (SpectraMax Plus384; Molecular Devices, Inc.).

Effects of Ca Concentration on Osteoblast Function: Ca-modified Eagle's MEM containing 100, 200, or 400 mg L^{-1} Ca was purchased from Nissui Pharmaceutical Co., Ltd. (Tokyo, Japan) and supplemented with 10% FBS, 100 μg mL^{-1} ascorbic acid and 5 mM β-glycerol phosphate for use as the osteogenic medium. Osteoblast-like stromal cells were cultured in standard α-MEM containing 10% FBS and, after 2 days, the medium was switched to the Ca-modified Eagle's MEM osteogenic medium. Three times per week, the culture medium was replaced by aspirating half of the supernatant and adding the same amount of new osteogenic medium. Five days after replacing the culture medium, the cells were stained for alkaline phosphatase (ALP) by the method of Yamamoto et al.[51] On Days 1 and 5 after replacing the culture medium, total RNA was collected to synthesise cDNA and real-time RT-PCR was performed as described above.

Evaluation of Calcification in Osteoblast-like and Fibroblast-like Cell Lines: The osteoblast-like cell line MC3T3-E1 (Riken, Ibaraki, Japan) and fibroblast-like cell lines NIH3T3 (Riken) and ST2 (Riken) were cultured as described for osteoblast-like stromal cells and, after 5 weeks of culture, were stained with alizarin to assess calcification.

Next, NIH3T3 and ST2 were cultured in α-MEM containing 10% FBS for 2 days. The medium was replaced with osteogenic medium containing 100 ng mL^{-1} rhBMP-2 (R&D Systems, Inc., Minneapolis, MN, USA) followed by the addition of MWCNTs or CB, or no carbon as a control. The cells were cultured for 3 weeks and stained with alizarin to assess calcification.

To investigate whether calcification in ST2 cells involved ALP, ALP activity was stimulated by culturing the cells with rhBMP-2 plus 0, 0.5, or 1.0 mM 3,4-dehydro-L-proline (DHP) (Sigma, St. Louis, MO, USA), an ALP inhibitor. First, ST2 cells were cultured in α-MEM containing 10% FBS for 2 days, and the medium was replaced with an osteogenic medium containing 100 ng mL^{-1} of rhBMP-2 plus the indicated concentration of DHP. Half of the medium was replaced 3 times per week. After culture for 1 week, ALP activity was quantified colourimetrically using a TRACP & ALP Assay Kit (Takara Bio Inc.) and ImmunoMini NJ-2300 (Nalge Nunc International, Tokyo, Japan).

Another set of cells were prepared as described above and 50 μg mL^{-1} of MWCNTs was added on Day 2 of culture. Cells were cultured for 3 weeks and stained with alizarin to assess calcification. The inhibitory effect of DHP on ALP was also determined by staining cells for ALP.

Statistical Analysis: All values are expressed as means ± s.d. Statistical analysis was performed using the Student's *t* test or analysis of variance followed by Tukey's post hoc test, as appropriate. Values of $P < 0.05$ were considered statistically significant. Each experiment was repeated at least three times, and similar results were obtained. SPSS software (version 14.0; SPSS Inc., Chicago, IL, USA) was used for all statistical analyses.

Acknowledgements

We thank T. Hanada and K. Kametani for their excellent assistance with this work. This research was supported by Program for Fostering Regional Innovation in Nagano, granted by MEXT, Japan; by a Grant-in-Aid for Scientific Research from the Ministry of Education, Science, Sports, and Culture, Japan; and the Japan Regional Innovation Strategy program by the Excellence of the Japan Science and Technology Agency.

Received: October 6, 2011
Revised: December 12, 2011
Published online: March 22, 2012

[1] S. Iijima, *Nature* **1991**, *354*, 56.
[2] A. Oberlin, M. Endo, T. J. Koyama, *Cryst. Growth* **1976**, *32*, 335.
[3] R. Van Noorden, *Nature* **2011**, *469*, 14.
[4] F. Xiong, A. D. Liao, D. Estrada, E. Pop, *Science* **2011**, *332*, 568.
[5] L. Qu, L. Dai, M. Stone, Z. Xia, Z. L. Wang, *Science* **2008**, *322*, 238.
[6] R. H. Baughman, A. A. Zakhidov, W. A. de Heer, *Science* **2002**, *297*, 787.
[7] F. Yang, C. Jin, D. Yang, Y. Jiang, J. Li, Y. Di, J. Hu, C. Wang, Q. Ni, D. Fu, *Europ. J. Cancer* **2011**, *47*, 1873.
[8] S. J. Singh, *Nanosci. Nanotechnol.* **2010**, *10*, 7906.
[9] A. Ruggiero, C. H. Villa, J. P. Holland, S. R. Sprinkle, C. May, J. S. Lewis, D. A. Scheinberg, M. R. McDevitt, *Inter. J. Nanomed.* **2010**, *5*, 783.
[10] P. Chaudhuri, R. Harfouche, S. Soni, D. M. Hentschel, S. Sengupta, *ACS Nano* **2010**, *4*, 574.
[11] A. A. Bhirde, V. Patel, J. Gavard, G. Zhang, A. A. Sousa, A. Masedunskas, R. D. Leapman, R. Weigert, J. S. Gutkind, J. F. Rusling, *ACS Nano* **2009**, *3*, 307.
[12] C. Arnould, T. I. Korányi, J. Delhalle, Z. J. Mekhalif, *Colloid Interf. Sci.* **2010**, *344*, 390.
[13] T. J. Webster, M. C. Waid, J. L. McKenzie, R. L. Price, J. U. Ejiofor, *Nanotechnology* **2004**, *15*, 48.
[14] T. Dvir, B. P. Timko, D. S. Kohane, R. Langer, *Nat. Nanotechnol.* **2011**, *6*, 13.
[15] P. A. Tran, L. Zhang, T. J. Webster, *Adv. Drug Deliver.Rev.* **2009**, *61*, 1097.
[16] L. Zhang, T. J. Webster, *Nano Today* **2009**, *4*, 66.
[17] A. Abarrategi, M. C. Gutiérrez, C. Moreno-Vicente, M. J. Hortigüela, V. Ramos, J. L. López-Lacomba, M. L. Ferrer, F. del Monte, *Biomaterials* **2008**, *29*, 94.
[18] B. S. Harrison, A. Atala, *Biomaterials* **2007**, *28*, 344.
[19] Y. Usui, K. Aoki, N. Narita, N. Murakami, I. Nakamura, K. Nakamura, N. Ishigaki, H. Yamazaki, H. Horiuchi, H. Kato, S. Taruta, Y. A. Kim, M. Endo, N. Saito, *Small* **2008**, *4*, 240.
[20] M. Bhattacharya, P. Wutticharoenmongkol-Thitiwongsawet, D. T. Hamamoto, D. Lee, T. Cui, H. S. Prasad, M. J. Ahmad, *Biomed. Mater. Res. A* **2011**, *96*, 75.
[21] S. Shao, S. Zhou, L. Li, J. Li, C. Luo, J. Wang, X. Li, J. Weng, *Biomaterials* **2011**, *32*, 2821.
[22] C. Lin, Y. Wang, Y. Lai, W. Yang, F. Jiao, H. Zhang, S. Ye, Q. Zhang, *Colloid. Surface. B* **2011**, *83*, 367.
[23] T. R. Nayak, L. Jian, L. C. Phua, H. K. Ho, Y. Ren, G. Pastorin, *ACS Nano* **2010**, *4*, 7717.
[24] M. Van der Zande, X. F. Walboomers, M. Brännvall, B. Olalde, M. J. Jurado, J. I. Alava, J. A. Jansen, *Acta Biomater.* **2010**, *6*, 4352.
[25] N. Saito, T. Okada, H. Horiuchi, N. Murakami, J. Takahashi, M. Nawata, H. Ota, K. Nozaki, K. Takaoka, *Nat. Biotechnol.* **2001**, *19*, 332.
[26] M. Vandrovcová, L. Bačáková, *Physiol. Res.* **2011**, *60*, 403.
[27] P. Ducy, T. Schinke, G. Karsenty, *Science* **2000**, *289*, 1501.
[28] P. Ducy, R. Zhang, V. Geoffroy, A. Ridall, G. Karsenty, *Cell* **1997**, *89*, 747.
[29] A. Yamaguchi, T. Ishizuya, N. Kintou, Y. Wada, T. Katagiri, J. M. Wozney, V. Rosen, S. Yoshiki, Biochem, *Biophys. Res. Commun.* **1996**, *220*, 366.